Theoretical Investigation of the 3,4-Ethylenedioxythiophene Dimer and Unsubstituted Heterocyclic Derivatives

Carlos Alemán*,† and Jordi Casanovas*,‡

Departament d'Enginyeria Química, E.T.S. d'Enginyers Industrials de Barcelona, Universitat Politècnica de Catalunya, Diagonal 647, Barcelona E-08028, Spain, and Departament de Química, Escola Politècnica Superior, Universitat de Lleida, c/Jaume II n° 69, Lleida E-25001, Spain

Received: October 2, 2003; In Final Form: December 18, 2003

The molecular geometry, torsional potential, and selected electronic properties (ionization potential and band gap) of the 3,4-ethylenedioxythiophene dimer in both neutral and doped (radical cation) states were investigated using quantum mechanical methods. Calculations were performed using the HF, B3LYP, B3PW91, MPW1PW91, and MP2 methods and the 6-31G(d), 6-31+G(d,p), and 6-311++G(d,p) basis sets. In all cases, calculations on the neutral and radical states were carried out considering the restricted and unrestricted formalisms, respectively. Results have been compared with experimental data when available. Furthermore, five derivatives of the 3,4-ethylenedioxythiophene dimer were built by changing the heteroatoms at both the five- and six-membered rings. Their conformational and electronic properties were studied using B3PW91/6-31+G(d,p) calculations. Results indicated that the material generated by interchanging the positions of the oxygen and sulfur atoms with respect to the parent compound presents very promising properties.

Introduction

The design of π-conjugated polymers with a small energetic separation between occupied and unoccupied levels was pioneered by Wudl et al.[1] two decades ago. Since then, this goal has attracted considerable attention because such materials are expected to present high electrical conductivities in both the neutral (undoped) and oxidized (doped) states. A very promising approach within this field is based on the modification by substitution of polymers with chemical and electrical stability, such as polythiophene.[2−5] Among the derivatives of polythiophene, poly(3,4-ethylenedioxythiophene), abbreviated PEDOT, showed a combination of interesting properties: low oxidation potential, low band gap, and remarkable stability, even in aqueous medium.[4,5] The structure of PEDOT is shown in Chart 1.

PEDOT, with dioxane rings fused onto thiophene rings, presents less steric hindrances than those encountered with disubstituted polythiophenes. The oxygen atoms, which are directly attached at the 3- and 4-positions, exert an electron-donating effect that reduces the band gap.[4,5] Thus, the electrochemical analysis indicated a band gap of 1.2 eV,[6] the conductivities measured for the polymer prepared electrochemically ranging from 10 to 100 S/cm.[7] Furthermore, such conductivities were stable for up to 1000 h at 120 °C. On the other hand, spectroscopic studies suggested that the electronic structure of neutral PEDOT is intermediate between that of the benzoid and the quinoid.[8] This behavior should indicate that the usual transition {benzoid structure} → {quinoid structure} during the doping process is not valid for PEDOT. This polymer has been shown to be useful as an antistatic material,[4c,5] as a solid electrolyte in capacitors,[7a,9] and as electrodes of biosensors

CHART 1: PEDOT

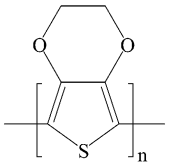

to amperometrically detect glucose.[10] In addition, this material presents a useful electrochromic behavior, that is, the ability to reversibly change color by altering the redox state, which is a consequence of its low oxidation potential.[4d,11] The color cycles between an opaque blue-black in the undoped state and a transmissive sky-blue in the oxidized state, which suggests its use as a cathodically coloring electrochromic material.[12]

Quantum-chemical calculations have been recently employed to investigate different aspects related to the structure and properties of PEDOT.[13−16] However, the number of such studies is still very scarce and, in some cases, the results provided are unclear. The geometric and electronic structure of neutral and doped oligomers containing *N* EDOT monomers, where *N* ranges from 1 to 10, was investigated using both HF/6-31G(d) and B3LYP/6-31G(d) calculations.[13,14] Results indicated that the ground state of neutral PEDOT is clearly benzoid, which is in marked disagreement with previous proposals based on spectroscopic data.[8] Regarding the singly and doubly positively charged compounds, Hartree−Fock (HF) and density-functional theory (DFT) led to different results. The first method localizes the positive charge around the center of the molecule, whereas the second one leads to delocalization of the charge all along the conjugated path. On the other hand, the properties of copolymers containing alternating fluorene−EDOT units[15] and 4-(dicyanomethylene)-4*H*-cyclopenta[2,1-*b*:3,4-*b*′]dithiophene−EDOT units[16] were investigated using semiempirical and DFT calculations, respectively. However, these studies were mainly

* E-mail: carlos.aleman@upc.es (C.A.); jcasanovas@quimica.udl.es (J.C.).
† Universitat Politècnica de Catalunya.
‡ Universitat de Lleida.

10.1021/jp0369600 CCC: $27.50 © 2004 American Chemical Society
Published on Web 01/31/2004

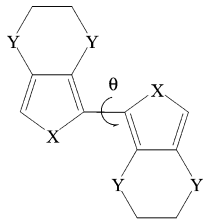

(**1**): X= S, Y= O
(**2**): X= O, Y= O
(**3**): X= O, Y= S
(**4**): X= S, Y= S
(**5**) X= N-H, Y= O
(**6**) X= N-H, Y= S

Figure 1. Chemical structure of the compounds investigated in this study. The inter-ring dihedral angle (θ) is indicated.

devoted to ascertain whether the donor−acceptor concept is useful for improving the electrical properties of conducting polymers.

In this work we exploit quantum-chemical calculations to provide a complete characterization of the molecular geometry, electronic structure, and torsional potential of neutral and doped (radical cation) EDOT dimer (**1**, Figure 1), which may be envisaged as the simplest model of PEDOT. These properties have been predicted using HF, MP2, and DFT calculations. Accordingly, an important aspect of our work is to propose a functional able to describe the electronic structure of neutral and doped PEDOT. We hope that the present results can help to clarify whether the electronic structure of the undoped polymer is benzoid, as was found in previous DFT studies,[13,14] or quinoid, as suggested by the spectroscopic data reported by some authors.[8] Furthermore, the strength of the theoretical methods was used to investigate the effects caused by the substitution of the heteroatoms in PEDOT in the above-mentioned properties. For this purpose, calculations were performed on five additional compounds (**2**−**6**), which are specifically displayed in Figure 1.

Methods

The calculations were performed at the "Centre de Supercomputació de Catalunya" (CESCA) using Gaussian 98.[17] Ab initio calculations were performed at the HF and MP2[18] levels of theory. On the other hand, different functionals were employed for DFT calculations. More specifically, we used the following three combinations: the Becke's three-parameter hybrid functional (B3)[19] with the Lee, Yang, and Parr (LYP)[20] expression for the nonlocal correlation (B3LYP); the same functional with the nonlocal correlation provided by Perdew and Wang (B3PW91);[21] and the modified Perdew−Wang exchange[22] with the PW91 gradient-corrected correlation (MPW1PW91).[21] As usual, the effect of doping was mimicked by considering the ionized species of the compound alone, without a counterion. However, we are aware that the assumption of ideal charge transfer between the dopant and the doped molecule could affect in some way the comparison with experimental results. In all cases, quantum-chemical calculations on the neutral state (closed-shell system) and the radical cation (open-shell system) were performed considering the restricted and unrestricted formalisms, respectively. The 6-31G(d)[23] and 6-31+G(d,p)[24] basis sets were used in geometry optimizations. Single-point calculations were performed in selected cases using the 6-311++G(d,p)[24] basis set.

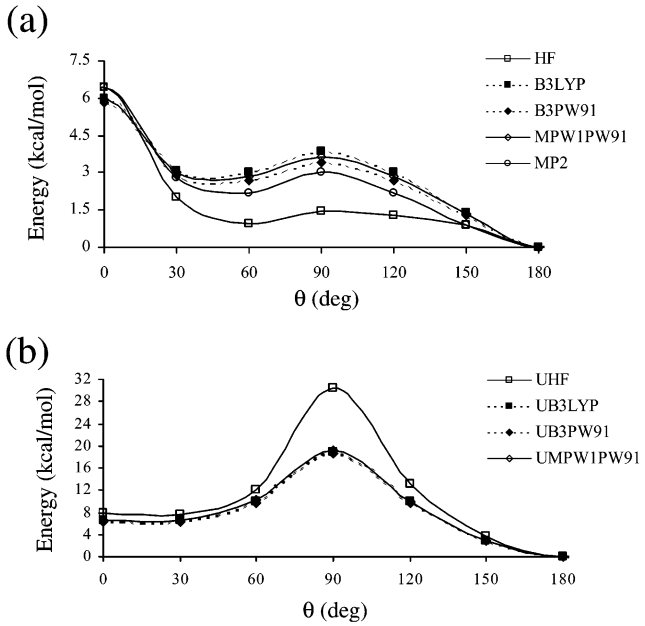

Figure 2. Potential energy curves for the internal rotation of **1** (a) and $\mathbf{1}^{\bullet+}$ (b) as a function of the inter-ring dihedral angle (θ). The methods used for geometry optimizations are indicated for each compound. Calculations were performed in all cases using the 6-31G-(d) basis set. Energies are relative to the global minimum.

To study the internal rotation, the torsional angle θ (Figure 1) was scanned in steps of 30° between $\theta = 180°$ (anti conformer) and $\theta = 0°$ (syn conformer). A flexible rotor approximation was used for all the compounds investigated. Thus, the structure in each point of the path was obtained from geometry optimization at a fixed θ value. The equilibrium geometries of each compound were fully optimized using a gradient method. All the minimum energy structures were characterized as such by calculating and diagonalizing the Hessian matrix and ensuring that they do not have any negative values.

Ionization potentials (IP) were estimated using the Koopman's theorem (KT),[25] that is, relating the IP to the energy of the HOMO (highest occupied molecular orbital), which according to the Janak's theorem can be also applied to DFT calculations.[26] However, more accurate IP values were obtained in selected cases using the energies of the fully relaxed neutral and ionized species. This approach, usually denoted ΔSCF, takes into account the relaxation energy of the ionized state, which can be calculated as the difference between the KT and ΔSCF IPs.[27] Finally, the energy gap (ϵ_g) was evaluated as the difference between the HOMO and LUMO (lowest unoccupied molecular orbital) energies. In an early work, Levy and Nagy[26b] showed that in DFT calculations ϵ_g can be correctly estimated using this procedure.

Results and Discussion

Neutral EDOT Dimer (1). The rotational profiles computed for **1** at the HF/6-31G(d), B3LYP/6-31G(d), B3PW91/6-31G-(d), MPW1PW91/6-31G(d), and MP2/6-31G(d) levels are displayed in Figure 2a. The energies and torsional angles of the minima and saddle points obtained by the different methods are compiled in the Supporting Information (Table S1). Surprisingly, the global minimum predicted by all the methods appears at $\theta = 180°$ (anti conformation), rather than at $\theta \approx 150°$ (anti−gauche conformation) as occurs for the thiophene dimer.[28] Furthermore, the anti−gauche conformation was also character-

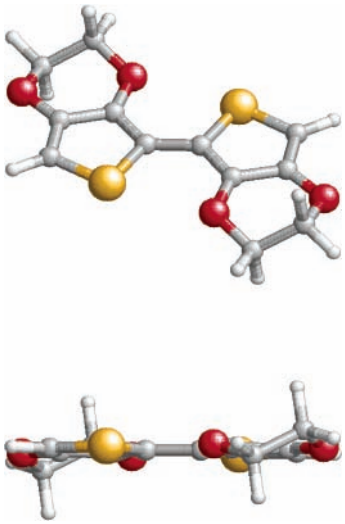

Figure 3. Molecular structure (two views) of the anti minimum obtained for **1** at the B3PW91/6-31G(d) level. The twist conformation of the fused dioxane rings is illustrated.

ized as the global minimum for isothianaphthene dimer,[2j] in which each unit is formed by the fusion of a benzene ring upon thiophene. Thus, values of $\theta = 132.9°$, 129.9°, and 126.5° were calculated at the HF/6-31G(d), B3PW91/6-31G(d), and MP2/6-31G(d) levels,[2j] respectively, indicating that the reduction of the angle θ alleviates the steric interactions induced by the benzene rings. Similarly, the anti−gauche conformation was predicted as the most stable for polypentafulvalenes, a family of polycyclic compounds in which the two fused rings of each unit are coplanar.[29] However, in **1** the repulsive contacts between each sulfur atom and the dioxane fused onto the neighboring thiophene are eliminated by the twist conformation of the six-membered rings. This conformation reduces the C−O−C bond angle increasing the distance between the sulfur and oxygen atoms. Figure 3 shows the anti minimum detected at the B3PW91/6-31G(d) level, in which the twist conformation is specifically displayed. Furthermore, as will be discussed below, the double bond character of the inter-ring bond is larger in **1** than in the thiophene dimer, enhancing the stability of the planar conformation in the former.

A local minimum appears for **1** at $\theta \approx 50°$ (syn−gauche conformation), which is about 2.0−2.6 kcal/mol less stable than the global minimum using the DFT and MP2 methods in conjunction with the 6-31G(d) basis set. Both minima are separated by the gauche−gauche barrier at $\theta = 90°$. This is unfavored by about 3.0−3.5 and 1.0−1.3 kcal/mol with respect to the anti and syn−gauche minima. Finally, the syn−gauche minimum and its degenerated state at $\theta \approx -50°$ are separated by the syn barrier ($\theta = 0°$), which is about 2.1−3.5 kcal/mol higher in energy than the gauche−gauche barrier.

Comparison between the HF curve and those obtained with the DFT and MP2 methods indicates that the former does not provide a precise representation of the torsional potential of **1**, which is due to the neglection of electron correlation effects. Thus, the energies of the syn−gauche and gauche−gauche conformations are underestimated by about 1 and 1.5 kcal/mol, respectively, by the noncorrelated method. Furthermore, the HF method provides the syn−gauche minimum at $\theta = 54.9°$, this value being at least 5° higher than that predicted by correlated methods. On the other hand, for the different functionals employed, the agreement with the MP2 profile evolves along the series B3LYP < MPW1PW91 < B3PW91. It should be emphasized that previous studies[2j,3a,30] indicated that the MP2/6-31G(d) method provides very accurate results not only for the thiophene dimer but also for its derivatives. We have thus chosen the B3PW91 functional to investigate the influence of the basis set in the rotational barrier of **1**, since it is the functional that affords energies and geometries closer to the MP2 results.

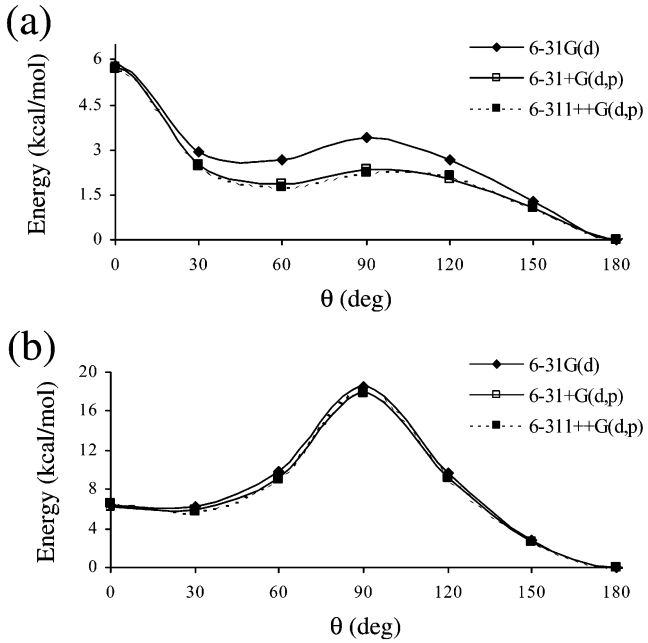

Figure 4. Potential energy curves for the internal rotation of **1** (a) and $\mathbf{1}^{\bullet+}$ (b) as a function of the dihedral angle θ using (U)B3PW91/6-31G(d) and (U)B3PW91/6-31+G(d,p) optimizations. The curves obtained using single-point calculations at the (U)B3PW91/6-311++G(d,p) level on geometries optimized at the (U)B3PW91/6-31+G(d,p) level are also displayed. Energies are relative to the global minimum.

TABLE 1: Inter-Ring Bond Length (*d*), Difference between the Inter-Ring Bond Lengths of the Global Minimum and the Gauche−Gauche Barrier (δ), Ionization Potential (IP) Estimated Using the Koopman's Theorem, and Energy Gap (ϵ_g) for 1 Obtained by Different Computational Methods

method	*d* (Å)	δ (Å)	IP (eV)	ϵ_g (eV)
HF/6-31G(d)	1.460	0.007	7.26	10.01
B3LYP/6-31G(d)	1.442	0.015	4.86	4.06
B3PW91/6-31G(d)	1.440	0.010	4.94	4.09
MPW1PW91/6-31G(d)	1.439	0.014	5.13	4.45
MP2/6-31G(d)	1.438	0.016	4.94	4.08
B3PW91/6-31+G(d,p)	1.441	0.014	5.16	4.04
B3PW91/6-311++G(d,p)			5.20	4.04

Figure 4a compares the rotational profiles derived from B3PW91/6-31G(d) and B3PW91/6-31+G(d,p) optimizations. Single-point energy calculations at the B3PW91/6-311++G(d,p) level were performed using the latter geometries, the resulting curve being also displayed in Figure 4a (see also Table S1). As can be seen, the relative energies of the nonplanar conformations are overestimated when diffuse functions are not considered. Thus, the 6-31G(d) basis set overestimates the energy of such conformations by about 25−45% with respect to the 6-311++G(d,p) one. However, the small difference found between the curves computed using the 6-31+G(d) and 6-311++G(d,p) basis sets indicates that the first one is sufficiently accurate in the case of **1**.

Table 1 shows the inter-ring bond length predicted by the different methods for the anti minimum. As expected, the bond length provided by the HF method is larger (∼0.02 Å) than the values obtained using correlated methods. It is worth noting that, independently of the computational procedure, the inter-ring bond length calculated for **1** is smaller than that reported

for the global minimum of 2,2′-bithiophene. Thus, the value predicted for 2,2′-bithiophene at the HF/6-31G(d), MP2/6-31G(d), and B3LYP/6-31G(d) levels was 1.465,[28a] 1.452,[31] and 1.448 Å,[31] respectively. This reduction, which is especially notable at the MP2/6-31G(d) level (0.014 Å), indicates that the contribution of the quinoid form to the electronic structure is larger for **1** than for 2,2′-bithiophene, in agreement with experimental observations.[8] This feature is reinforced by the parameter δ, which corresponds to the difference between the inter-ring bond lengths of the global minimum and the gauche−gauche barrier (Table 1). The value of δ predicted for 2,2′-bithiophene at the MP2/6-31G(d) (0.009 Å) level[31] was 0.007 Å smaller than that computed for **1** at the same level of theory. Thus, the transformation suffered by the electronic structure of the global minimum when the system evolves toward the benzoid structure of the barrier is more pronounced for **1**.

The influence of the computational method on the IP and ϵ_g is analyzed in Table 1. The IP, which indicates whether a given acceptor (p-type dopant) is capable of ionizing the compound, was estimated using the KT. As can be seen, the IP and ϵ_g values calculated using the HF method are notably overestimated with respect to those obtained using the MP2 and DFT schemes. This is because electron correlation is not included in the former. In this context, the values provided by the B3PW91 functional are almost identical to those derived at the MP2 level, even though an excellent agreement is also found between the latter method and the other functionals. On the other hand, the improvement of the basis set is accompanied by a very small change in ϵ_g (0.05 eV) indicating that this electronic property is not influenced by the addition of diffuse and polarization functions. However, the extension of the basis set from 6-31G(d) to 6-31+G(d,p) produces a change of 0.22 eV in the IP, whereas the 6-31+G(d,p) and 6-311++G(d,p) basis sets provide very similar results.

The ϵ_g predicted at the B3PW91/6-31+G(d,p) level (4.04 eV) is considerably overestimated with respect to the experimental data, the electrochemical and optical band gaps reported for PEDOT being 1.2[6] and 1.5−1.7[4f,11,32] eV. However, caution should taken with these experimental measures because the optical band gap, which is approximated by the longest wavelength absorption or emission band, should be larger than the electrochemical band gap that is estimated from the difference between the first oxidation and reduction potentials. The overestimation of the theoretical values must be partially attributed to the small number of EDOT monomers considered in the present calculations. The reduction of the gap with increasing chain length is a well-known behavior that has been shown in numerous theoretical studies of π-conjugated polymers,[33,15] including PEDOT.[16] Thus, this effect was shown by previous calculations employing the B3PW91 functional with the Stevens−Bach−Krauss pseudopotentials,[34] and split valence plus polarization basis sets predicted an ϵ_g of 2.06 eV for PEDOT, whereas values of 6.43 and 4.68 eV were provided for EDOT and the dimer, respectively,[16] Thus, a reduction of about 50% was detected when going from the dimer to the polymer. We have also checked the influence of the number of EDOT units on the ϵ_g. For this purpose, additional calculations were performed at the B3PW91/6-31+G(d,p) level on compounds containing one and three EDOT units. The ϵ_g of the optimized structures was 5.65 and 3.30 eV, respectively, confirming that the gap decreases when the amount of EDOT units increases. However, the fact that the gas-phase DFT calculations yield values directly comparable with experiments in condensed media indicates that the ϵ_g is notably underestimated by this technique. On the other hand, the IP predicted for PEDOT by Salzner and Köse[16] was 4.38 eV, which is in agreement with our B3PW91/6-31+G(d) estimation for **1** (5.16 eV). The IP calculated for compounds with one and three EDOT units was 6.09 and 4.71 eV, respectively.

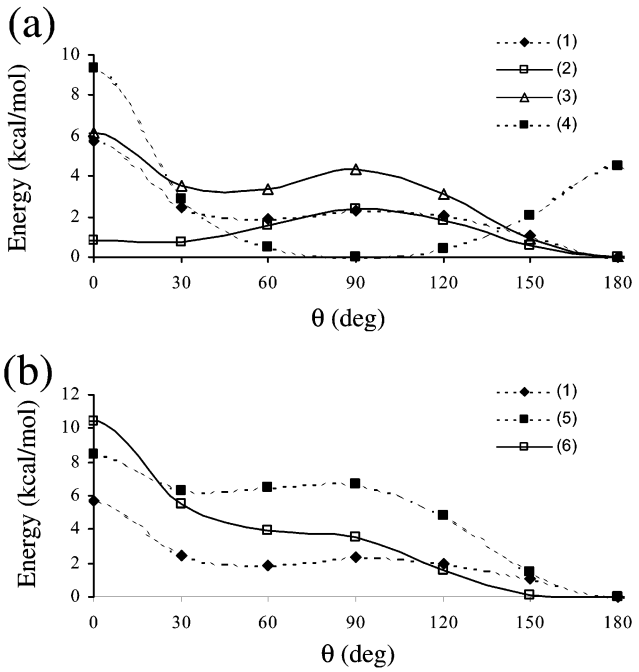

Figure 5. Potential energy curves for the internal rotation as a function of the dihedral angle θ computed at the B3PW91/6-31+G(d,p) level: (a) **2**−**4**; (b) **5** and **6**. For comparison, the rotational profile of **1** calculated at the same level of theory is also displayed.

Substitution of the Heteroatoms at the Neutral EDOT Dimer (2−6). The influence of the sulfur and oxygen atoms on the molecular and electronic structure of **1** was investigated by considering five additional compounds, in which the heteroatoms of the former have been changed. The chemical structure of the generated compounds is displayed in Figure 1. As can be seen, in **2** the sulfur atom of each thiophene ring has been replaced by an oxygen atom, in **3** the positions of the sulfur and oxygen atoms have been interchanged, and in **4** the oxygen atoms of the dioxane rings have been substituted by sulfur atoms. The evolution of the B3PW91/6-31+G(d,p) energy for **2**−**4** as a function of θ is displayed in Figure 5a. To have a better understanding of the effects induced by the changes at the heteroatoms, the curve of **1** computed at the same level of theory is also displayed. The relative energies and the torsional angles of the minima and saddle points are given in the Supporting Information (Table S2), whereas the inter-ring distances, δs, IPs, and ϵ_g values are listed in Table 2.

The most stable conformation for **2** corresponds to the anti conformation, the gauche−gauche barrier being unfavored by 1.9 kcal/mol. This value is consistent with that of **1** at the same level of theory (2.3 kcal/mol). The more remarkable differences between **1** and **2** only involve the syn−gauche minimum and the syn barrier. Thus, the local minimum for **1** and **2** arises when θ is 50.3° and 28.8°, respectively. Furthermore, this structure is 0.7 kcal/mol less favored than the anti conformation for **2**, whereas an energy difference of 1.7 kcal/mol appears for **1**. Accordingly, the substitution of the thiophene by furane affects both the planarity and stability of the syn−gauche minimum. This is because the interactions between the heteroatoms are less repulsive for **2** than for **1**, that is, the oxygen atom is smaller than the sulfur one. Similarly, the energy of

TABLE 2: Inter-Ring Bond Length (d), Difference between the Inter-Ring Bond Lengths of the Global Minimum and the Gauche−Gauche Barrier (δ), Ionization Potential (IP) Estimated Using the Koopman's Theorem, and Energy Gap (ϵ_g) Obtained for 1−6 Using B3PW91/6-31+G(d,p) Calculations

compound	d (Å)	δ (Å)	IP (eV)	ϵ_g (eV)
1	1.441	0.014	5.16	4.04
2	1.431	0.011	4.96	4.28
3	1.431	0.017	5.12	3.99
4	1.461[a]	*b*	5.82	4.81
5	1.435	0.020	4.56	4.56
6	1.446	*b*	4.88	4.29

[a] The inter-ring bond length corresponds to the gauche−gauche conformation, which is the global minimum of **4**. [b] No barrier was detected at the gauche−gauche conformation.

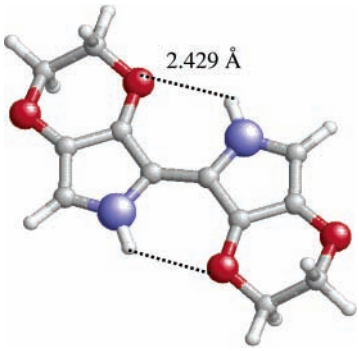

Figure 6. Molecular structure of the global minimum obtained for **5** using B3PW91/6-31+G(d) optimizations. Intermolecular hydrogen bonding distances (in Å) are displayed.

the syn barrier is considerably higher for **1** than for **2**, that is, 4.8 kcal/mol. On the other hand, a detailed comparison between the inter-ring distances, δs, IPs, and ϵ_g values calculated for **1** and **2** indicates that the modification at the five-membered ring does not have any relevant effect on the electronic structure. Thus, although the inter-ring distance, δ, and IP are slightly smaller for **2** (0.010 Å, 0.003 Å, and 0.20 eV, respectively), the value of ϵ_g is slightly smaller for **1** (0.24 eV).

The rotational profile obtained for **3** shows a destabilization of the syn−gauche minimum and the gauche−gauche barrier with respect to **1** (0.7 and 1.1 kcal/mol, respectively). Obviously, this is a consequence of the repulsive interactions induced by the heteroatoms located at the six-membered rings, which are stronger for **3** than for **1**. On the other hand, the relative energy of the syn barrier is almost identical for **3** and **1**. In this case, the diminishment in the repulsion produced by the substitution at the five-membered ring compensates for the enhancement in the repulsion generated by the change at the six-membered ring. Inspection of Table 2 indicates that both the IP and ϵ_g of **3** are slightly lower than those of **1** (0.04 and 0.05 eV, respectively), suggesting that the interchange of the sulfur and oxygen positions produces a small improvement in the electronic properties. This interesting result combined with the increase of the relative energies of the gauche−gauche barrier and the syn−gauche local minimum with respect to **1** indicates that polymers based on **3** should be viewed as promising conducting materials.

The case of **4** appears very different. The lowest energy minimum corresponds to the gauche−gauche conformation, which presents a dihedral angle $\theta = 85.8°$. The syn and anti planar conformations are 9.3 and 4.5 kcal/mol less stable than the gauche−gauche conformation, respectively. These conformational preferences are the consequence of the repulsive interactions originating from the sulfur atoms, which are maxima in the syn conformation. Comparison between the relative energies predicted for **2** and **4** indicates that the S···S interactions are 8.4 and 4.5 kcal/mol more unfavored than the O···O ones in the syn and anti conformations, respectively. These interactions are notably reduced when the rings adopt a perpendicular arrangement. This situation produces a loss of inter-ring π interactions with respect to the other compounds investigated, which is reflected in an enlargement of the inter-ring bond length (0.02 Å). Furthermore, the IP and ϵ_g predicted for **4** increase with respect to those calculated for **1** by 0.66 and 0.77 eV (13% and 19%, respectively).

In compounds **5** and **6** the two thiophene rings were replaced by pyrrole rings, the only difference between these two compounds being the heteroatoms contained in the six-membered rings: oxygen and sulfur for the former and the latter, respectively. There is a notable difference between the conformational properties of the pyrrole-containing compounds and those of **1** (Figure 5b and Table S2). This is the stabilization of the anti minimum with respect to all the other conformations, which is due to the formation of an intramolecular hydrogen bond between the N−H group of each pyrrole ring and the closest heteroatom of the neighboring six-membered ring. These interactions, which are illustrated in Figure 6 for **5**, are more attractive for this compound than for **6** as revealed by the H···X (X = O or S) distances: $d_{H\cdots O} = 2.429$ Å and $d_{H\cdots S} = 2.434$ Å. Accordingly, the destabilization of the syn conformation with respect to the anti one is larger for **6** than for **5** by almost 2 kcal/mol. Furthermore, the relative energy of the syn conformation is higher for the pyrrole-containing compounds than for **1**−**3**. On the other hand, it should be noted that the presence of intramolecular hydrogen bonds also affects the syn−gauche minimum and the gauche−gauche barrier. The energies of the local minimum and the energy barrier are almost identical for **5**, whereas for **6** no local minimum is detected at the syn−gauche conformation (Table S2).

The data displayed in Table 2 indicate that the stabilization of the planar anti conformation is not accompanied by an increase of the π conjugation. Thus, the inter-ring distance is similar or even larger than that calculated for the thiophene- and furane-containing compounds. Regarding the electronic structure of **5** and **6**, the formation of intramolecular interactions affects both the IP and the ϵ_g. The HOMO and the LUMO are less stable in the pyrrole-containing compounds than in **1**. As a consequence, the IP and ϵ_g increase by about 0.3−0.5 eV with respect to **1**. Finally, it should be mentioned that in all the compounds investigated, the six-membered rings adopt a twist conformation like that displayed in Figure 3 for **1**.

Doped Dimers ($\mathbf{1}^{\bullet+}$ and $\mathbf{3}^{\bullet+}$). Calculations were performed for the cation radical $\mathbf{1}^{\bullet+}$ using spin-unrestricted HF (UHF) and DFT (UB3LYP, UB3PW91, and UMPW1PW91) methods. It should be mentioned that UHF wave functions are plagued with contamination of higher spin states,[34] whereas spin-unrestricted DFT solutions have been found to suffer much less from this problem.[35] Unrestricted MP2 calculations were not performed in this case because they involve a huge amount of computer time. The rotational profiles obtained for $\mathbf{1}^{\bullet+}$ through UHF/6-31G(d), UB3LYP/6-31G(d), UB3PW91/6-31G(d), and UMPW1PW91/6-31G(d) optimizations are displayed in Figure 2b, whereas the relative energies and dihedral angles of the more important conformations are listed in the Supporting Information (Table S3). It is worth noting that the three DFT methods provide very similar results, whereas energies derived from UHF calculations are overestimated, especially for the gauche−gauche barrier.

CHART 2: Quinoid Structure of $1^{\bullet+}$

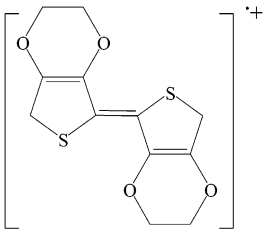

TABLE 3: Inter-Ring Bond Length (d), Difference between the Inter-Ring Bond Lengths of the Global Minimum and the Gauche−Gauche Barrier (δ), Ionization Potential (IP) Estimated Using the Koopman's Theorem, and Energy Gap (ϵ_g) for $1^{\bullet+}$ Obtained by Different Computational Methods

method	d (Å)	δ (Å)	IP (eV)	ϵ_g (eV)
UHF/6-31G(d)	1.389	0.070	12.35	8.48
UB3LYP/6-31G(d)	1.400	0.031	9.37	1.75
UB3PW91/6-31G(d)	1.398	0.031	9.50	1.79
UMPW1PW91/6-31G(d)	1.395	0.032	9.71	2.16
UB3PW91/6-31+G(d,p)	1.399	0.030	9.61	1.78
UB3PW91/6-311++G(d,p)			9.64	1.78

Full geometry optimizations of $\mathbf{1}^{\bullet+}$ lead to two minima: the anti ($\theta = 180°$) and the syn−gauche ($\theta \approx 23°$) conformations. The tendency of the latter minimum, which is about 6 kcal/mol less favored than the former, to adopt a planar arrangement is fully consistent with the quinoid structure expected for $\mathbf{1}^{\bullet+}$. Furthermore, the gauche−gauche barrier is about 15 kcal/mol higher than that obtained for **1**. This energy increment clearly indicates that the conversion from one minimum to the other involves the rotation around a double bond in the quinoid structure of $\mathbf{1}^{\bullet+}$ (Chart 2). The formation of a quinoid structure is more evident when the inter-ring bond lengths of $\mathbf{1}^{\bullet+}$, which are shown in Table 3, are compared with those of **1** (Table 1). Thus, the inter-ring distance is about 0.04 Å larger for the latter. On the other hand, the syn conformation is slightly more destabilized ($\sim$ 0.6 kcal/mol) with respect to the anti minimum for $\mathbf{1}^{\bullet+}$ than for **1**. This must be attributed to the reduction of the inter-ring bond length in the former, which produces an enhancement of the repulsive interactions between the heteroatoms.

For consistency with the calculations displayed above for **1**, the influence of the basis set on the conformational preferences of $\mathbf{1}^{\bullet+}$ was investigated using the B3PW91 functional. The resulting rotational profiles are displayed in Figure 4b, and Table 3 summarizes the more important results related to the electronic properties. As can be seen, almost identical rotational profiles were obtained with the 6-31G(d), 6-31+G(d), and 6-311++G(d,p) basis sets. Thus, the relative energy of the syn−gauche and gauche−gauche conformations decreases by only 6% and 3%, respectively, when the basis set extends from 6-31G(d) to 6-311++G(d,p), that is, 0.4 and 0.5 kcal/mol, respectively. Similar conclusions can be extracted from Table 3: the influence of the basis set on both the IP and ϵ_g is negligible.

A comparison between the electronic properties of $\mathbf{1}^{\bullet+}$ and **1** indicates that, as expected, the ϵ_g is considerably lower for the former than for the later. Thus, DFT calculations predict that doping reduces the gap by about half, whereas the reduction obtained by HF calculations is only 15%. On the other hand, the IP of the doped species is almost two times higher than that of the neutral compound indicating that the energy needed for the formation of the bipolaron is considerably larger than that employed for the polaron.

On the other hand, we have investigated the molecular and electronic properties of the cation radical $\mathbf{3}^{\bullet+}$ using UB3PW91/6-31+G(d,p) calculations. As stated previously, the values of the IP and ϵ_g predicted for **3** are smaller than those obtained for the parent compound **1** (Table 2), and therefore, the importance of this derivative is especially relevant. Figure 7 compares the rotational profile calculated for $\mathbf{3}^{\bullet+}$ with that predicted for $\mathbf{1}^{\bullet+}$ at the same level of theory (see also Table S4 of the Supporting Information). As can be seen, the relative energy of the gauche−gauche barrier is 1.4 kcal/mol higher for $\mathbf{1}^{\bullet+}$ than for $\mathbf{3}^{\bullet+}$. This must be attributed to the interactions between the heteroatoms contained in the five-membered rings, which are less repulsive for the oxygen atoms than for the sulfur atoms. The same explanation should be used to justify the instability of the planar syn conformation that is 0.3 kcal/mol higher for $\mathbf{1}^{\bullet+}$ than for $\mathbf{3}^{\bullet+}$. However, the most remarkable result of the conformational profile obtained for $\mathbf{3}^{\bullet+}$ is the absence of a syn−gauche local minimum, which points out the remarkable tendency of this compound to adopt planar conformations.

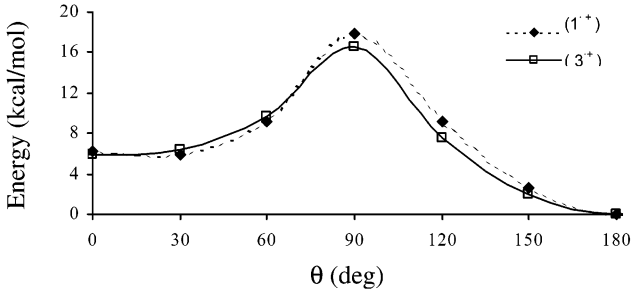

Figure 7. Potential energy curve for the internal rotation as a function of the dihedral angle θ computed at the UB3PW91/6-31+G(d,p) level for $\mathbf{3}^{\bullet+}$. For the sake of comparison, the rotational profile of $\mathbf{1}^{\bullet+}$ calculated at the same level of theory is also displayed.

TABLE 4: Inter-Ring Bond Length (d), Difference between the Inter-Ring Bond Lengths of the Global Minimum and the Gauche−Gauche Barrier (δ), Ionization Potential (IP) Estimated Using the Koopman's Theorem, and Energy Gap (ϵ_g) of $1^{\bullet+}$ and $3^{\bullet+}$ Obtained through UB3PW91/6-31+G(d,p) Calculations[a]

compound	d (Å)	δ (Å)	IP (eV)	ϵ_g (eV)
$\mathbf{1}^{\bullet+}$	1.399	0.030	9.61	1.78
$\mathbf{3}^{\bullet+}$	1.394	0.027	9.28	1.56

[a] Syn, $\theta = 0°$; gauche−gauche barrier, $\theta = 90°$.

Table 4 shows the IP and ϵ_g values calculated for $\mathbf{3}^{\bullet+}$. As can be seen, the values predicted for both properties are smaller than those obtained for the radical cation of the parent compound. This situation is similar to that detected for neutral dimers from a qualitative point of view. However, a quantitative comparison between the results displayed in Tables 2 and 4 reveals that the differences between the two compounds are considerably greater in the doped state than in the undoped one. Thus, the IP and ϵ_g differences obtained for the radical cations are 0.33 and 0.22 eV, respectively, whereas such values were only 0.04 and 0.05 eV for the neutral dimers.

Comparison between the IPs Predicted by the KT and the ΔSCF Approaches. It should be emphasized that the IPs displayed in Tables 3 and 1 for $\mathbf{1}^{\bullet+}$ and **1**, respectively, were derived using the KT. Therefore, they should be considered as rough estimations since no relaxation is considered for the final state of the ionization process. To investigate the influence of the relaxation energy (ϵ_r), the IP was recalculated for **1** though the ΔSCF approach using the energies computed for $\mathbf{1}^{\bullet+}$. Results are displayed in Table 5. As expected, the KT overestimates the IP by about 30% within the HF formalism. The relaxation of the molecular and electronic structures of the ionized state

TABLE 5: Comparison between the Ionization Potential (in eV) Estimated Using the Koopman's Theorem (KT) and the ΔSCF Approach for 1 by Different Computational Methods[a]

method	KT[b]	ΔSCF	ϵ_r
HF/6-31G(d)	7.26	5.52	−1.74
B3LYP/6-31G(d)	4.86	6.24	+1.38
B3PW91/6-31G(d)	4.94	6.33	+1.39
MPW1PW91/6-31G(d)	5.13	6.35	+1.22
B3PW91/6-31+G(d,p)	5.16	6.49	+1.33
B3PW91/6-311++G(d,p)	5.20	6.52	+1.32

[a] The relaxation energy (ϵ_r, in eV) corresponds to the difference between the KT and the ΔSCF values. [b] From Table 1.

provides a reduction of 1.74 eV in the IP. A completely different behavior was derived from DFT calculations. Thus, the IP obtained using the KT was systematically underestimated with respect to that predicted by the ΔSCF approach. Furthermore, the IP obtained using the latter method shows a very small dependence on both the functional and the basis set, ranging from 6.24 to 6.52 eV. The systematic underestimation of the IP by the KT was also detected by Barrio et al.[36] in a recent DFT study devoted to the investigation of aromatic systems constituted by fused rings. These authors found that the KT (evaluated in the neutral form) does not correctly describe the effects associated with the *annulation*, especially those related to the polarizability of the fused rings.

Similarly, the energies of **3** and $\mathbf{3}^{\bullet+}$ allowed the estimation of the IP of the former dimer using the ΔSCF approach. This value was 6.42 eV at the UB3PW91/6-31+G(d,p) level, indicating that the KT underestimated the IP of **3** by 1.30 eV (20%). This overestimation was almost identical to that predicted for **1** at the same level of theory, that is, 1.33 eV (20%). This is a very reasonable result since the above-mentioned annulation effects are expected to be similar in **1** and **3**. Furthermore, the ΔSCF approach predicts that the IP of **3** is smaller than that of **1** by 0.07 eV, this amount being quite close to that obtained using the KT (0.04 eV).

Summary and Conclusions

A detailed quantum mechanical study of **1** and $\mathbf{1}^{\bullet+}$ has been performed in order to gain some insight into the conformational and electronic properties of longer molecules based on EDOT units. Fully optimized torsional potentials have been calculated for **1** at the HF/6-31G(d), B3LYP/6-31G(d), B3PW91/6-31G(d), MPW1PW91/6-31G(d), MP2/6-31G(d), and B3PW91/6-31+G(d,p) levels. Furthermore, the geometries provided by the latter method were used for single-point calculations at the B3PW91/6-311++G(d,p) level. A comparison among the results derived from all these calculations indicated that the B3PW91/6-31+G(d,p) method is suitable to study the properties of EDOT-based compounds. The most stable conformation is always calculated to correspond to the fully planar anti structure. A second local minimum is found for a syn−gauche conformation with a θ of about 50°. The energy difference between the two minima is about 2 kcal/mol, which indicates that the abundance of the latter is expected to be negligible. Furthermore, the gauche−gauche barrier is unfavored by about 2.5 kcal/mol. The contribution of the quinoid form to the electronic structure is larger for **1** than for 2,2′-bithiophene, in agreement with experimental observations. The IP and ϵ_g calculated for **1** are larger than those experimentally measured for PEDOT, which is due to the small number of EDOT units considered in the calculations. This was confirmed by performing selected calculations on compounds containing one and three EDOT units.

Calculations on $\mathbf{1}^{\bullet+}$ were performed at the UHF/6-31G(d), UB3LYP/6-31G(d), UB3PW91/6-31G(d), UMPW1PW91/6-31G(d), UB3PW91/6-31+G(d,p), and UB3PW91/6-311++G(d,p) levels. In all cases the rotational profiles were consistent with a quinoid electronic structure. Thus, the high value detected for the relative energy of the gauche−gauche barrier is consistent with the double character of the inter-ring bond. The minima for $\mathbf{1}^{\bullet+}$ are the anti and syn−gauche conformations, the latter being about 6 kcal/mol less favored than the former. Thus, the local minimum is notably less favored in the doped state than in the neutral state. On the other hand, a comparison between the electronic properties of **1** and $\mathbf{1}^{\bullet+}$ points out that the ionization is accompanied by: (1) an increase of the IP and (2) a reduction of the ϵ_g.

Conformational and electronic properties of five compounds, which were derived from **1** by changing the heteroatoms at both the five- and six-membered rings, were calculated at the B3PW91/6-31+G(d,p) level. Results have been discussed taking into account the chemical nature of the heteroatoms. A very noticeable result was obtained for **3**, in which the positions of the sulfur and oxygen atoms are interchanged with respect to **1**. The IP and ϵ_g of this compound are smaller than those of **1** in both the neutral and doped states. Accordingly, molecules based on **3** should be considered as promising conducting materials.

Acknowledgment. The authors are indebted to the Centre de Supercomputació de Catalunya (CESCA) and the Centre Europeu de Paral·lelisme de Barcelona (CEPBA) for use of their computational facilities. This work has been supported by MCYT with Grant MAT2003-00251.

Supporting Information Available: Dihedral angles, atomic coordinates, and energies of the conformations investigated for all the compounds. This material is available free of charge via the Internet at http://pubs.acs.org.

References and Notes

(1) Wudl, F.; Kobayashi, M.; Heeger, A. J. *J. Org. Chem.* **1984**, *49*, 3382.

(2) (a) Brédas, J. L.; Heegerer, A. J.; Wudl, F. *J. Chem. Phys.* **1986**, *85*, 4673. (b) Colaneri, N.; Kobayashi, M.; Heeger, A. J.; Wudl, F. *Synth. Met.* **1986**, *14*, 45. (c) Lee, Y. S.; Kertesz, M. *J. Chem. Phys.* **1988**, *88*, 2609. (d) Lee, Y. S.; Kertesz, M.; Elsenbaumer, R. L. *Chem. Mater.* **1990**, *2*, 526. (e) Kuerti, J.; Surján, P. R.; Kertesz, M. *J. Am. Chem. Soc.* **1991**, *113*, 9865. (f) Quatrocchi, C.; Lazzaroni, R.; Brédas, J. L.; Zamboni, R.; Taliani, C. *Macromolecules* **1993**, *26*, 1260. (g) Hanack, M.; Mangold, K.-M.; Röhrig, U.; Maichle-Mössmer, C. *Synth. Met.* **1993**, *60*, 199. (h) Hanak, M.; Schmid, U.; Röhrig, U.; Toussaint, J. M.; Adant, C.; Brédas, J. L. *Chem. Ber.* **1993**, *126*, 1487. (i) Ksatner, J.; Kuzmany, H.; Vegh, D.; Landl, M.; Cuff, L.; Kertesz, M. *Macromolecules* **1995**, *28*, 2922. (j) Viruela, P. M.; Viruela, R.; Ortí, E.; Brédas, J. L. *J. Am. Chem. Soc.* **1997**, *119*, 1360.

(3) (a) De Oliveira, M. A.; Duarte, H. A.; Pernaut, J.-M.; De Almeida, W. B. *J. Phys. Chem. A* **2000**, *104*, 8256. (b) Demanze, F.; Cornil, J.; Garnier, F.; Horowitz, G.; Valat, P.; Yaasar, A.; Lazzaroni, R.; Brédas, J. L. *J. Phys. Chem. B* **1997**, *101*, 4553. (c) DiCésare, N.; Belletête, M.; Raymond, F.; Leclerc, M.; Durocher, G. *J. Phys. Chem. A* **1998**, *102*, 2700. (d) Zhang, Q. T.; Tour, J. M. *J. Am. Chem. Soc.* **1998**, *120*, 5355.

(4) (a) Apperloo, J.; Groenendaal, L. B.; Verheyen, H.; Jayakannan, M.; Janssen, R. A.; Dkhissi, A.; Beljonne, D.; Lazzaroni, R.; Brédas, J. L. *Chem.—Eur. J.* **2002**, *8*, 2384. (b) Yu, J.; Holdcroft, S. *Chem. Mater.* **2002**, *14*, 3705. (c) Jonas, F.; Schrader, L. *Synth. Met* **1991**, *41*, 831. (d) Pei, Q.; Zuccarello, G.; Ahlskog, M.; Inganäs, O. *Polymer* **1994**, *35*, 1347. (e) Sakmeche, N.; Aaron, J. J.; Fall, M.; Aeiyach, S.; Jouni, M.; Lacroix, J. C.; Lacaze, P. C. *Chem. Commun.* **1996**, 2723. (f) Sankaran, B.; Reynolds, J. R. *Macromolecules* **1997**, *30*, 2582.

(5) Goenendaal, L.; Jonas, F.; Freitag, D.; Pielartzik, H.; Reynolds, J. R. *Adv. Mater.* **2000**, *12*, 481.

(6) (a) Huang, H.; Pickup, P. G. *Chem. Mater.* **1998**, *10*, 2212. (b) Ahonen, H. J.; Lukkari, J.; Kankare, J. *Macromolecules* **2000**, *44*, 6787. (c) Fu, Y.; Cheng, H.; Elsenbaumer, R. L. *Chem. Mater.* **1997**, *9*, 1720.

(7) (a) Heywang, G.; Jonas, F. *Adv. Mater.* **1992**, *4*, 116. (b) Winter, I.; Reese, C.; Hormes, J.; Heywang, G.; Jonas, F. *Chem. Phys.* **1995**, *194*, 207.

(8) (a) Garreau, S.; Louarn, G.; Buisson, J. P.; Froyer, G.; Lefrant, S. *Macromolecules* **1999**, *32*, 6807. (b) Garreau, S.; Duvail, J. L.; Louarn, G. *Synth. Met.* **2001**, *125*, 325. (c) Lapkowski, M.; Pron, A. *Synth. Met.* **2000**, *110*, 79.

(9) (a) Jonas, F.; Heywang, G. *Electrochim. Acta* **1994**, *39*, 1345. (b) Kudoh, Y.; Akami, K.; Matsuya, Y. *Synth. Met.* **1999**, *102*, 973. (c) Ghosh, S.; Inganäs, O. *Adv. Mater.* **1999**, *11*, 1214.

(10) (a) Kros, A.; van Hövell, S. W. F. M.; Sommerdijk, N. A. J. M.; Nolte, R. J. M. *Adv. Mater.* **2001**, *13*, 1555. (b) Kros, A.; Nolte, R. J. M.; Sommerdijk, N. A. J. M. *J. Polym. Sci., Part A: Polym. Chem.* **2002**, *40*, 738.

(11) Sotzing, G. A.; Reynolds, J. R.; Steel, P. J. *Chem. Mater.* **1996**, *8*, 882.

(12) (a) Dietrich, M.; Heinze, J.; Heywang, G.; Jonas, F. *J. Electroanal. Chem.* **1994**, *369*, 87. (b) Gustafsson, J. C.; Liedberg, B.; Inganäs, O. *Solid State Ionics* **1994**, *69*, 145.

(13) Dkhissi, A.; Louwet, F.; Groenendaal, L.; Beljonne, D.; Lazzaroni, R.; Brédas, J. L. *Chem. Phys. Lett.* **2002**, *359*, 466.

(14) Dkhissi, A.; Beljonne, D.; Lazzaroni, R.; Louwet, F.; Groenendaal, L.; Brédas, J. L. *Int. J. Quantum Chem.* **2002**, *91*, 517.

(15) Cornil, J.; Gueli, I.; Dkhissi, A.; Sancho-García, J. C.; Hennebicq, E.; Calbert, J. P.; Lemaur, V.; Beljonne, D.; Brédas, J. L. *J. Chem. Phys.* **2003**, *118*, 6615.

(16) Salzner, U.; Köse, M. E. *J. Phys. Chem. B* **2002**, *106*, 9221.

(17) Frisch, M. J.; Trucks, G. W.; Schlegel, H. B.; Scuseria, G. E.; Robb, M. A.; Cheeseman, J. R.; Zakrzewski, V. G.; Montgomery, J. A., Jr.; Stratmann, R. E.; Burant, J. C.; Dapprich, S.; Millam, J. M.; Daniels, A. D.; Kudin, K. N.; Strain, M. C.; Farkas, O.; Tomasi, J.; Barone, V.; Cossi, M.; Cammi, R.; Mennucci, B.; Pomelli, C.; Adamo, C.; Clifford, S.; Ochterski, J.; Petersson, G. A.; Ayala, P. Y.; Cui, Q.; Morokuma, K.; Malick, D. K.; Rabuck, A. D.; Raghavachari, K.; Foresman, J. B.; Cioslowski, J.; Ortiz, J. V.; Stefanov, B. B.; Liu, G.; Liashenko, A.; Piskorz, P.; Komaromi, I.; Gomperts, R.; Martin, R. L.; Fox, D. J.; Keith, T.; Al-Laham, M. A.; Peng, C. Y.; Nanayakkara, A.; Gonzalez, C.; Challacombe, M.; Gill, P. M. W.; Johnson, B. G.; Chen, W.; Wong, M. W.; Andres, J. L.; Head-Gordon, M.; Replogle, E. S.; Pople, J. A. *Gaussian 98*, revision A.7; Gaussian, Inc.: Pittsburgh, PA, 1998.

(18) Møller, C.; Plesset, M. S. *Phys. Rev.* **1934**, *46*, 618.

(19) Becke, A. D. *J. Chem. Phys.* **1993**, *98*, 1372.

(20) Lee, C.; Yang, W.; Parr, R. G. *Phys. Rev. B* **1993**, *37*, 785.

(21) Perdew, J. P.; Wang, Y. *Phys. Rev.* **1992**, *45*, 13244.

(22) Adamo, C.; Barone, V. *J. Chem. Phys.* **1998**, *108*, 664.

(23) Hariharan, P. C.; Pople, J. A. *Chem. Phys. Lett.* **1972**, *16*, 217.

(24) Frich, M. J.; Pople, J. A.; Krishnam, R.; Binkley, J. S. *J. Chem. Phys.* **1984**, *80*, 3264.

(25) Koopmans, T. *Physica* **1934**, *1*, 104.

(26) (a) Janak, J. F. *Phys. Rev.* **1978**, *8*, 7165. (b) Levy, M.; Nagy, Á. *Phys. Rev.* **1999**, *59*, 1687.

(27) (a) Casanovas, J.; Ricart, J. M.; Rubio, J.; Illas, F.; Jiménez-Mateos, J. M. *J. Am. Chem. Soc.* **1996**, *118*, 8071. (b) Bagus, P. S.; Illas, F.; Casanovas, J.; Jiménez-Mateos, J. M. *J. Electron. Spectrosc.* **1997**, *83*, 151.

(28) (a) Alemán, C.; Juliá, L. *J. Phys. Chem.* **1996**, *100*, 1524. (b) Kofranek, M.; Kovar, T.; Lischka, H.; Karpfen, A. *J. Mol. Struct. (THEOCHEM)* **1991**, *259*, 181. (c) Quattrocchi, C.; Lazzaroni, R.; Brédas, J. L. *Chem. Phys. Lett.* **1993**, *208*, 120. (d) Hernández, V.; López-Navarrete, J. T. *Synth. Met.* **1996**, *76*, 221.)

(29) Hong, S. Y. *Chem. Mater.* **2000**, *12*, 495.

(30) Ortí, E.; Viruela, P. M.; Sánchez-Marín, J.; Tomás, F. *J. Phys. Chem.* **1995**, *99*, 4955.

(31) Alemán, C.; Domingo, V. M.; Fajarí, L.; Juliá, L.; Karpfen, A. *J. Org. Chem.* **1998**, 1041.

(32) (a) Roncali, J.; Akoudad, S. *Synth. Met.* **1998**, *93*, 111. (b) Kumar, A.; Reynolds, J. R. *Macromolecules* **1996**, *29*, 7629.

(33) (a) Salzner, U.; Lagowski, J. B.; Pickup, P. G.; Poirier, R. A. *J. Comput. Chem.* **1997**, *18*, 1943. (b) Nobutoki, H.; Koezuka, H. *J. Phys. Chem.* **1996**, *100*, 6451. (c) Ehrendorfer, Ch.; Karpfen, A. *J. Phys. Chem.* **1995**, *99*, 10196. (d) Ehrendorfer, Ch.; Karpfen, A. *J. Phys. Chem.* **1994**, *98*, 7492.

(34) Stevens, W.; Basch, H.; Krauss, M. *J. Chem. Phys.* **1984**, *81*, 6026.

(35) Löwdin, P.-O. *Phys. Rev.* **1995**, *97*, 1509.

(36) Barrio, L.; Catalán, J.; de Paz, J. L. G. *Int. J. Quantum Chem.* **2003**, *91*, 432.